

Supporting Information

Crystallinity and Defect State Engineering in Organo-Lead

Halide Perovskite for High-Efficiency Solar Cells

Baohua Wang^{a,b}, King Young Wong^b, Shangfeng Yang^a and Tao Chen^{a*}

a. Department of Materials Science and Engineering, Key Laboratory of Materials for Energy Conversion, University of Science and Technology of China, 96 Jinzhai Road, Hefei, 230026, Anhui, China.

b. Department of Physics, The Chinese University of Hong Kong, Shatin, N.T., Hong Kong, China.

Corresponding Author

*E-mail: tchenmse@ustc.edu.cn

Materials

All the chemicals were purchased from Sigma/Aldrich unless otherwise stated. The PEDOT:PSS aqueous solution employed in this work is Clevios AI 4083. PC₇₁BM, BCP and C₆₀ were bought from Lumtec. MAI was synthesized with hydroiodic acid and methyl ammonia solution according to the reported method.^[1] The FTO coated glass substrate has a square resistance of 14 Ω/□ with transparency of 80% over the visible spectrum.

Effect of Precursor Ratios on the Solvent Annealing Method

For the one-step spin-coated film with the precursor containing equal molar content of PbI₂ and MAI, there is no much difference in the morphology and crystallinity between the thermally and pyridine solvent annealed films, as shown in Figure S1 and S2. Both films show branchlike structures and relatively poor crystalline nature. This can be explained according to the reaction kinetics as we previously proposed.^[2] Usually, PbI₂ and MAI react quickly in the solution and the film has already solidified after the spin coating process. So the solvent annealing strategy has little effect on the morphology of the films prepared from equimolar precursor.

Another widely adopted precursor for preparing MAPbI₃ film contains PbCl₂ and MAI with a molar ratio of 1:3. The annealing process usually takes nearly 1 hour at 100 °C, which is longer than the ternary system due to the slow release of the Cl-containing compound. The pyridine-solvent annealed film prepared with the 1:3 precursors shows very low surface coverage on the substrate (Figure S1). The low coverage is possibly due to the high crystallization process induced dewetting. The slow reaction is accompanied by the release of chlorine and the solvent is likely to cause volume change in the film, leaving pinholes. In this regard, the ternary precursor containing PbI₂, PbCl₂ and MAI with a molar ratio of 0.5:0.5:2 is essential here to maintain a high coverage and good crystallinity due to the regulation of reaction rate and release of the pyridine vapor.

PL decay kinetics fitting

The PL decay kinetics of both the pyridine annealed and thermally annealed perovskite samples showed double-exponential decay mode within the first several hundred nanoseconds after the pulse pumping with a laser of 532 nm in wavelength. The data were fitted with the double-exponential decay function in the form of $y = A_1 * \exp(-x/t_1) + A_2 * \exp(-x/t_2)$, where y represents the normalized PL intensity and x is the time. The lifetime of the charge carriers corresponds to the time when the PL intensity decays to 1/e of the initial value. A fast and a slow time constant were obtained for both films. The pyridine solvent annealed film presented a fast lifetime of 26 ns and a slow lifetime of 117 ns and the values for the thermally annealed film were 24 ns and 65 ns, respectively. We attributed the fast decay to the surface recombination and the slow one to the bulk recombination. The charge lifetime in the bulk of the film is 1.8 times longer for the solvent annealed perovskite which confirms its good quality with less non-radiative recombination centres within the film.

Supporting figures

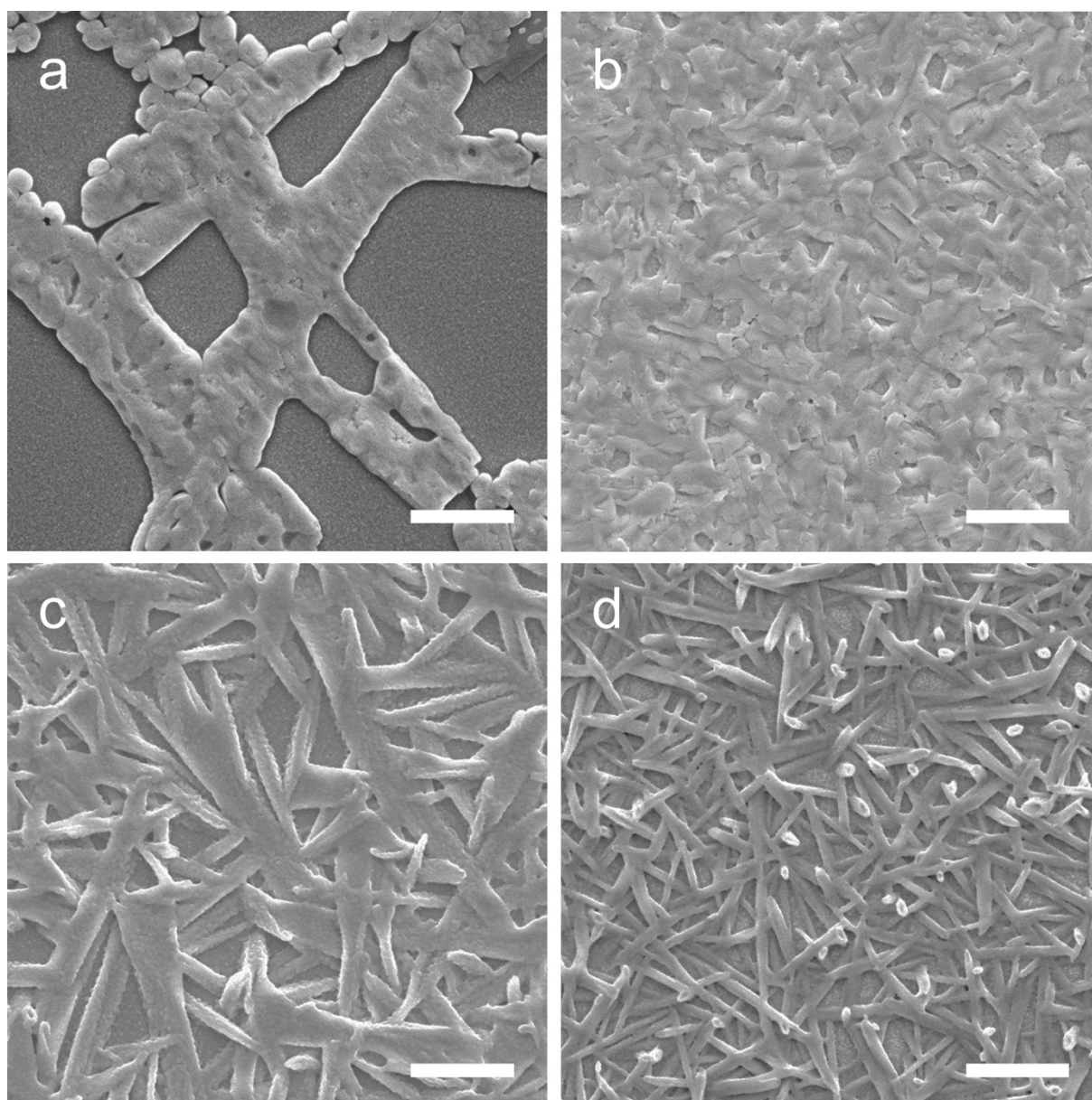


Figure S1. SEM images of the pyridine solvent annealed (a,c) and thermally annealed (b, d) perovskite films with the precursor containing 3:1 molar ratio of MAI and PbCl_2 (a, b) and equimolar of MAI and PbI_2 (c, d). Scale bars represent 5 μm .

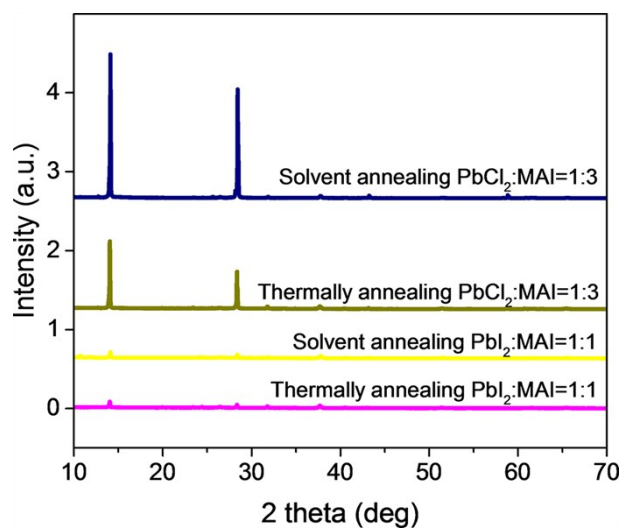


Figure S2. XRD patterns of the pyridine solvent annealed and thermally annealed perovskite films prepared with precursors containing equimolar of MAI and PbI₂ or 3:1 molar ratio of MAI and PbCl₂.

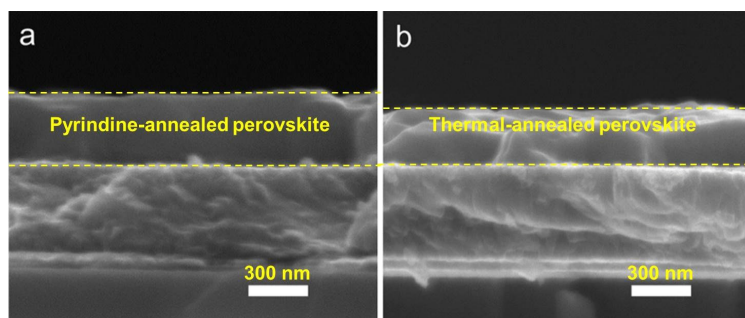


Figure S3 The cross-section-viewed SEM images of the solvent annealed (a) and thermal annealed (b) perovskite films.

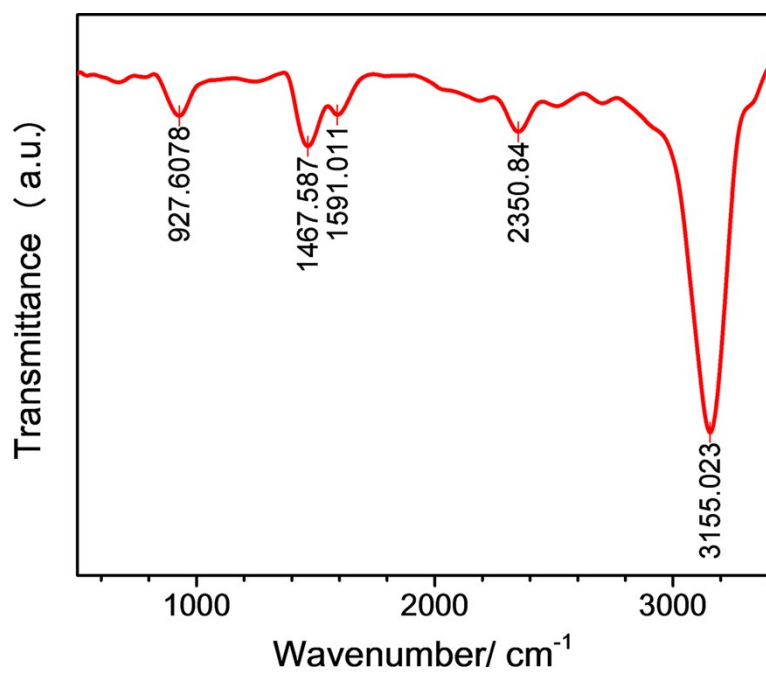


Figure S4. The FTIR spectrum of the perovskite film prepared with the pyridine solvent annealing method.

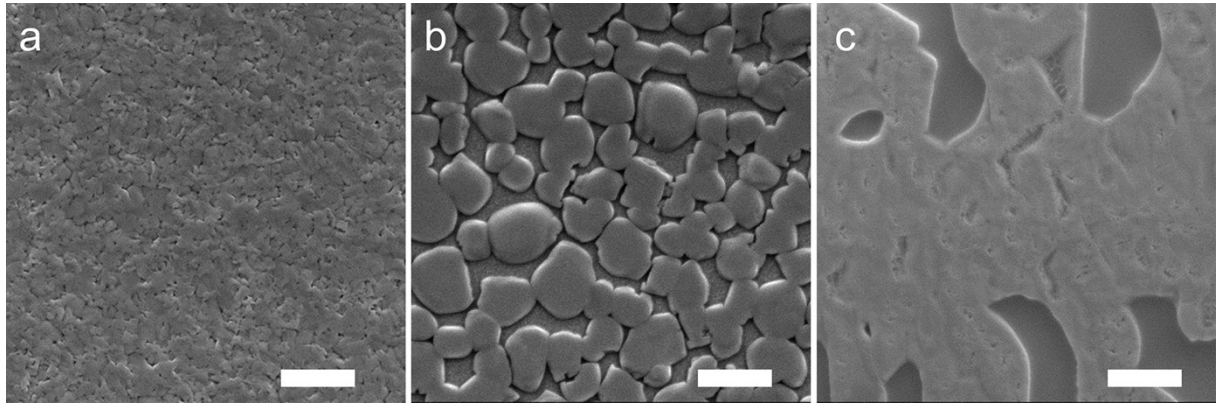


Figure S5. SEM images of the perovskite films prepared with the ternary precursor (MAI: PbI_2 : PbCl_2 = 2: 0.5: 0.5) annealed in THF (a), DMF (b) and DMSO (c) vapors. Scale bars represent 5 μm .

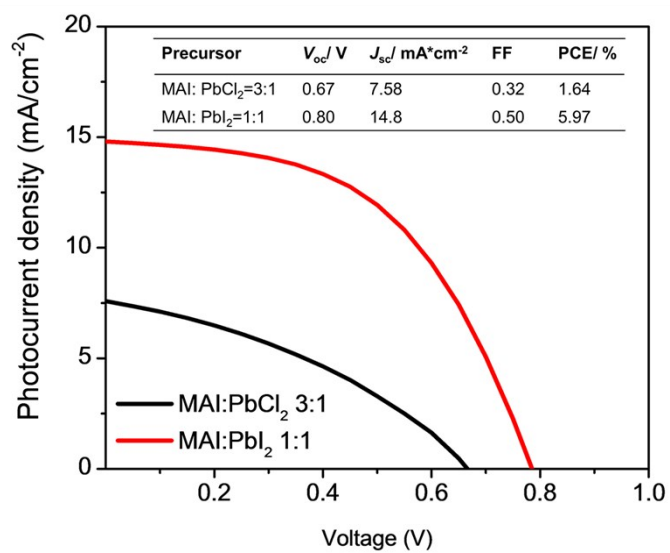


Figure S6. *J-V* response of the solar cells based on pyridine solvent annealed binary precursors

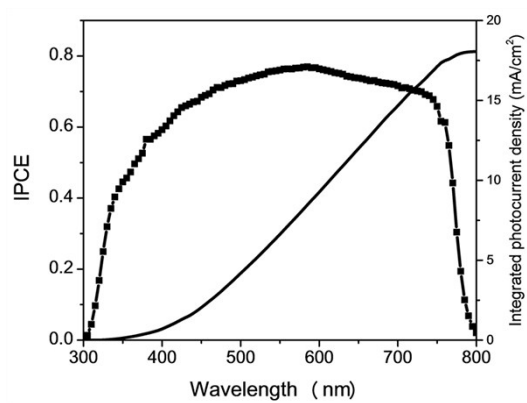


Figure S7. IPCE of a typical solar cell prepared from the pyridine solvent annealing method and the integrated short-circuit photocurrent density.

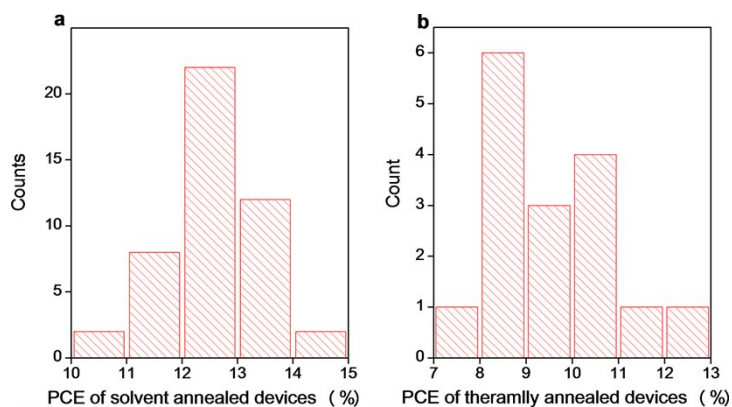


Figure S8. Statistics on the PCE of perovskite solar cells based on pyridine solvent annealed films (a) and thermally annealed films (b). The deviation for the solvent annealed devices and thermally annealed devices are 0.8% and 1.3%, respectively.

References

- 1 Kim, H. S.; Lee, C. R.; Im, J. H.; Lee, K. B.; Moehl, T.; Marchioro, A.; Moon, S. J.; Humphry-Baker, R.; Yum, J. H.; Moser, J. E.; Gratzel, M. and Park, N. G. *Sci. Rep.* **2012**, *2*, 591.
- 2 Wang, B.; Wong, K. Y.; Xiao, X. and Chen, T. *Sci. Rep.* **2015**, *5*, 10557.